

Enhancing Concrete Damage Detection through Ultrasonic Rebound Measurements and Deep Learning Techniques

Suzheng Zhao

Lecturer, School of Naval Architecture and Marine Engineering, Jiangsu Shipping College, Nantong 226010, China,
Email: zhaosz@jssc.edu.cn (corresponding author).

Project Management

Received December 13, 2023; received revision December 23, 2023; accepted March 13, 2024
Available online September 27, 2024

Abstracts: Due to the construction industry's rapid growth, concrete is now the standard building material used in new construction. In recent days, the development of the construction industry has focused heavily on how to maintain and identify the concrete structure of some older buildings. However, conventional concrete damage identification lacks precision and accuracy. Therefore, this work suggests an ultrasonic rebound enhancement approach based on deep learning. In order to detect concrete damage, the new algorithmic model measures the concrete data using the ultrasonic rebound technique and then analyses it using deep learning. By utilizing the improved Genetic Particle Swarm Optimization algorithm (GA-PSO) combined with the Back Propagation Neural Network, an improved GA-PSO-BP long-term concrete ultrasonic rebound comprehensive strength measurement model was established. The experimental results show that the improved GA-PSO-BP algorithm has a lower root mean square error than the conventional algorithm, which is lower than the Back Propagation neural network 0.008 and lower than the Genetic Algorithm-Back Propagation algorithm 0.001, and a higher accuracy rate than the Back Propagation algorithm model 0.07 and higher than the Genetic Algorithm-Back Propagation algorithm model 0.02. As a result, the improved GA-PSO-BP algorithm performs more precisely and accurately than the conventional approach. This study has practical applications for practitioners in the construction industry. The high accuracy and precision of the new algorithm render it an effective tool for identifying structural damage in old concrete buildings, which provides more reliable data support for maintenance efforts. This not only generates novel methods for enhancing concrete damage detection but also contributes to the sustainable development of the construction industry.

Keywords: Concrete damage detection, deep learning, ultrasonic rebound, improved algorithm.

Copyright © Journal of Engineering, Project, and Production Management (EPPM-Journal).
DOI 10.32738/IEPPM-2024-0030

1. Introduction

In engineering structural monitoring, concrete is a common and vital building material. It is imperative to detect concrete damage accurately and promptly to ensure the structure's reliability and safety (Jesús et al., 2021). The non-destructive testing method of the ultrasonic rebound plays a crucial role in evaluating the quality and degree of damage to concrete structures. However, conventional rebound techniques depend on operator skills and experience, leading to inadequate precision and accuracy (Peng et al., 2021). This study presents the application of deep learning technology to identify and quantitatively evaluate concrete damage in an automated and intelligent manner using neural networks' pattern recognition and data learning capabilities (Pan and Yang, 2020). The traditional ultrasonic rebound method faces limitations due to subjective factors and operator practical experience, which pose challenges in providing precise damage detection results under complex damage conditions. This research introduces deep learning techniques and employs extensive data to train neural network models, thus enhancing the accuracy and robustness of damage detection (Karve et al., 2020). Training and optimizing deep learning models and applying them to the field of ultrasonic rebound detection solves the limitations of traditional damage detection methods and improves the reliability and universality of detection. The main objective of this study is to explore a deep learning-based method for ultrasonic rebound measurement to enhance the accuracy and reliability of concrete damage detection (CDD). This study comprises four parts. The four sections of this study are as

follows: Section one provides an overview of research achievements both domestically and internationally. Section two presents a new model that was constructed to improve the deep learning algorithm. Section three analyzes the accuracy and other characteristics of the new model. Section 4 contains summarizes the research and briefly elaborates on the experimental results and future research directions.

2. Related Works

With the advancement of modern science, concrete is being used in construction on an increasing basis. As a result, determining the life, age, and degree of damage of concrete has become a crucial area for research. Numerous experts and academics have conducted extensive research on this topic. Lin and Scherer (2020) thought that the CDD of bridges is an important means of detection of the bridge building in use. In this study, a better concrete inspection method was proposed. The new method uses an advanced detection system that can respond to the data of the vehicles passing through the bridge and the bridge itself, and at the same time analyze the structure of the bridge. The experimental findings demonstrated that the new method outperformed the conventional method in determining the severity of concrete deterioration in bridges. Zhang et al (2020). in detecting the damage level of concrete in bridges found that traditional detection techniques built on the basis of neural networks can be limited by the data and the detector. Therefore, a new detector for physical detection was proposed, the new detector uses a new learning transfer method using new training weights. Bhowmick and Nagarajaiah (2020) found that the use of real-time automated detection was able to solve the problem of multiple cracks in detecting the extent of crack damage on the surface of the concrete. The principal component analysis method was able to detect cracks at different times. The experimental use of the method was also validated in the inspection of the concrete. The results of the experiments showed that the novel method, which can identify and track various fracture locations and moments, is a very useful detection technique. Gao and colleagues (2022) identified issues with the resolution level when using the traditional concrete damage imaging method. Consequently, they enhanced the imaging method resulting in the ability to examine spatial resolution and reconstruct spectral signals. The authors' findings have implications for improving CDD techniques. The experimental results demonstrated that the new method was able to achieve an increase in spatial resolution through damage imaging detection of concrete even when using instruments with reduced resolution.

Qi and Chen (2022) believed that the traditional CDD method will have detection failure, which will lead to the deterioration of the detection effect, so a new damage detection and crack analysis method is proposed on the traditional hierarchical analysis method, and a new damage detection system is built. The findings of the hierarchical analysis can be calculated, and their weights determined using the new method. According to the experimental findings, the novel approach offered greater detection sensitivity, greater detection speed, and higher detection accuracy. Yin et al. (2021) proposed a new damage detection technique after finding that the frequency generated by the pump wave is limited by the excitation limit, which leads to the reduction of the sensitivity of concrete detection. The new technique had lower power and was capable of detecting minor concrete damage. Nasery et al. (2020) found a new method of concrete detection in the experimental and identification detection of concrete; the new method is able to extract data from the concrete data in the conventional state and is able to determine the degree of damage to the data of concrete in the case of spring coefficient change. The experimental results showed that the new method had higher accuracy and higher recognition of the degree of concrete damage compared to the conventional method. The concrete structure of composite materials lacked a damage detection method. Through static simulation data and damage location, this novel approach can identify the concrete damage degree. The experimental findings showed that the novel approach can enhance concrete testing's sensitivity and enable the detection of the degree of damage to composite concrete structures.

In conclusion, even though many experts and academics have already attained a significant amount of research findings in the study of CDD, the research method still lacks sufficient accuracy and sensitivity. The current research is still focused on how to increase the accuracy and sensitivity of the CDD method. Therefore, this research will start from improving the accuracy and sensitivity of CDD method to study the problem.

3. Modelling of CDD by DL-based UR Assay

This chapter is to provide an overview of the determination principle of the UR determination method and how to use the UR determination method to determine concrete damage data. The new improved hybrid algorithm model is also built by combining three traditional DL algorithm models and the advantages of the new algorithm are described.

3.1. Determination of Concrete Damage by UR Method

The ultrasonic rebound comprehensive method combines the rebound and ultrasonic methods for non-destructive quality detection of concrete. Surface strength is measured with a rebound instrument, while internal conditions are determined using ultrasonic instruments. Concrete strength is predicted based on velocity values and rebound results. This method enhances detection accuracy and reliability compared to using only rebound or ultrasound. The rebound method refers to the use of rebounders to hit the concrete surface, using the elasticity of concrete to achieve a method of testing the strength of concrete. In practice, the working principle of the rebound instrument is to use the rebound needle on the rebound instrument to hit the concrete, so that the rebound needle is impacted by the elastic deformation, and then fed back to the rebound instrument in the system to test the impact by the size of the force to judge the strength of the concrete (Fang et al., 2020). The rebound instrument consists of rebound needle, spring, force receiving device, the main system and other components. The rebound needle is mainly responsible for the rebound instrument force transmission work, the received force transmission; spring is responsible for the transmission of the force further transmission to the rebound instrument, the force receiving device is responsible for receiving the rebound force, the main system is responsible for the analysis of

the force measured out of the concrete strength. The workflow of the rebound instrument can be expressed by Eq. (1) (Scherr and Grosse, 2020).

$$\Delta E = \frac{1}{2}KL^2 - \frac{1}{2}KX^2 \quad (1)$$

In Eq. (1), ΔE represents the change in potential energy before and after impact, K represents the stiffness strength of the spring, X represents the distance of spring rebound, and L represents the tensile length of the spring. Different outcomes will follow from the use of rebounders as the concrete structure varies, and there will also be specific requirements for the performance of the rebounders and the choice of parameters. The ultrasonic testing method can assess concrete performance using ultrasonic waves. An ultrasonic device emits pulse waves and reads data within the concrete to analyze its state. As shown in Eq. (2) (Zima and Krajewski, 2022).

$$V_p = \sqrt{\frac{\lambda + 2\mu}{\rho}} = \sqrt{\frac{E}{\rho} \cdot \frac{1 - \sigma}{(1 - 2\sigma)(1 + \sigma)}} \quad (2)$$

In Eq. (2), V_p denotes the velocity of the ultrasonic pulse, λ denotes the Lamé elastic constant, ρ denotes the density, σ denotes the Poisson's ratio, and E denotes the Young's modulus quantity. Since the composition of concrete is divided into two parts, the aggregate part and the cement stone, the ultrasonic pulse will be viewed as propagating through both parts. The propagation equation is shown in Eq. (3).

$$\frac{1}{v_b} = \frac{V_a}{v_a} + \frac{V_m}{v_m} \quad (3)$$

In Eq. (3), v_b represents the propagation speed of ultrasonic waves in cement, v_m represents the propagation speed of ultrasonic waves in concrete, V_a represents the relative volume size of aggregate, v_a represents the propagation speed of ultrasonic waves in aggregate, and V_m represents the relative volume size of cement. However, in practice, the mixing of cement will interfere with the ultrasonic waves in operation, resulting in detection errors, so the UR method is used to detect the concrete based on the combination of rebound and ultrasonic methods. The advantage of the UR method is that it can detect the surface strength of the concrete, but also can use ultrasonic waves to detect the internal structure of the concrete (Zima and Krajewski, 2022). Compared with the single detection method UR testing has higher precision and detection accuracy. However, the test range of this method is only applicable to the strength test of concrete within the age of 5 years, and other methods need to be used for the detection of concrete with a long age. Eq. (4) is the long age of concrete strength derivation equation (Van Steen et al., 2021).

$$f_{cm}(t) = \beta_\alpha(t)f_{cm} \quad (4)$$

In Eq. (4), $f_{cm}(t)$ denotes the average value of concrete strength at time t , f_{cm} denotes the strength of concrete against compression at the age of 27 days, $\beta_\alpha(t)$ denotes the coefficient expression of concrete at time t , and t denotes the age of concrete. The variation curve of concrete strength is shown in Eq. (5) (Van Steen et al., 2021).

$$f_{cu,i}^c = 0.0286v_i^{1.999}R_i^{1.155} \quad (5)$$

In Eq. (5), $f_{cu,i}^c$ denotes the value of the conversion unit of concrete strength, v_i denotes the representative value of the concrete when testing the rebound, and R_i denotes the representative value of the ultrasonic pulse in the testing interval. When the rebound value of concrete is obtained by ultrasonic pulse testing, the purpose of testing different test points can be achieved by using petroleum jelly to fit the plane of concrete and the plane of tester. Eq. (6) is the expression for calculating the average value tested at three test points (Znidaric et al., 2020).

$$v = \frac{l}{(t_1 + t_2 + t_3) / 3} \quad (6)$$

In Eq. (6), v denotes the value of ultrasonic pulse in the testing interval, l denotes the testing distance at different points in the testing interval, and t_1, t_2, t_3 denotes the acoustic time value at different testing points. When using the UR test method to detect the degree of damage and strength of concrete, it is able to achieve a comprehensive detection of

concrete with an age of up to 5 years, which is more meaningful than the traditional rebound and ultrasonic tests (Znidaric et al., 2020).

3.2. Research on CDD Algorithm Based on DL Improvement Algorithm

Deep learning algorithms utilize Artificial Neural Networks (ANN) to simulate the working principles of human brain neurons for pattern recognition and learning, making them a type of machine learning. Technical term abbreviations are explained upon first usage. The algorithms consist of Multilayer Perceptron (MLP), Recurrent Neural Networks (RNN), Genetic Algorithm (GA), Particle Swarm Optimization (PSO), and Back Propagation Neural Network (BPNN), which focus on concrete loss detection and global search abilities. For the purpose of algorithm optimization and enhancement, GA, PSO algorithm and BPNN with strong global search ability are selected. One of the DL techniques, BPNN, analyzes the concrete test data using the inputs of signal data and changes in neuron function to obtain the output value and expected value of the function network (Znidaric et al., 2020). As shown in Fig. 1, the learning procedure of BPNN is depicted.

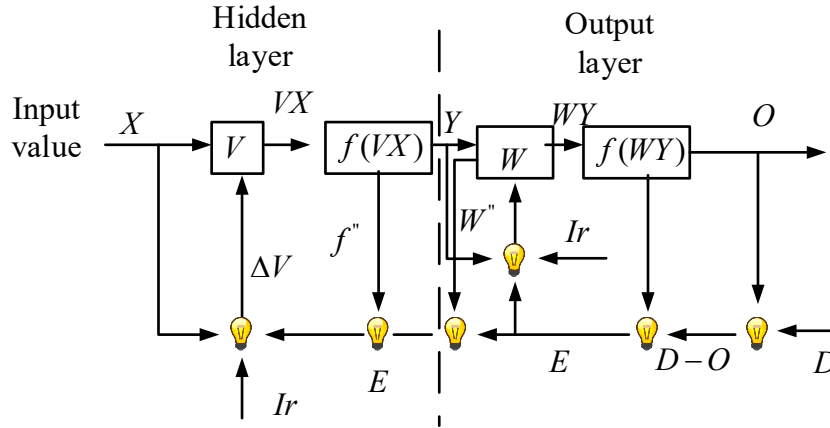


Fig. 1. BPNN learning process

In Fig. 1, the learning process of the BPNN is a unique data processing process. It can transform the degree of matching between input and output data into a nonlinear mapping problem, and then increase the accuracy of the mapping after gradient reduction and other ways. BPNN is mainly achieved through the backpropagation of the calculation results and error of the data calculation process, by the equation shown in Eq. (7) to process the data forward calculation of the implicit layer of the equation (Znidaric et al., 2020).

$$Y_j = f_1\left(\sum_{i=1}^n V_{ij} X_i\right) \quad (7)$$

Eq. (7) shows that f_1 denotes the transformation function of the hidden layer, X is the input data, equation is the input data at the i th time, V denotes the expression of the weight matrix of the hidden layer in the neural network, equation is the weight matrix of the j th neuron and the input data at the i th time. The equation expression for the output layer is shown in Eq. (8) (Lin et al., 2020).

$$O_k = f_2\left(\sum_{j=1}^m W_{kj} Y_j\right) \quad (8)$$

In Eq. (8), f_2 represents the transformation function of the output layer, Y represents the computed output value of the implicit layer, and equation represents the result at the j th implicit layer; O represents the result computed by the neurons of the data in the output layer, and equation represents the computed result at the k th layer; W represents the expression of the weight matrix of the output of the implicit layer, and equation represents the weight matrix of the k th neuron and the j th input data.

GA is an algorithmic model to simulate biological evolution, GA in solving the actual problem is through the selection of the problem data, and then the simulation of biological evolution on the data to achieve the analysis of the problem data parsing. As shown in Eq. (9), it is the expression of the equation of GA at the mutation operation (Lin et al., 2020).

$$\begin{aligned} P'_{c1} &= -(\alpha - 1)P_{c2} + \alpha P_{c1} \\ P'_{c2} &= -(\alpha - 1)P_{c1} + \alpha P_{c2} \end{aligned} \quad (9)$$

In Eq. (9), P'_{c1} and P'_{c2} denote the number of data completed because of gene crossover, P_{c1} and P_{c2} denote the number of individuals selected for gene crossover, and α denotes a random number in 0-1. When the genetic reference is conducted, individuals in each generation experience mutations in their genes as well as cross-overs during inheritance. This convergence through mutation leads to the continuous improvement of the algorithm, ultimately achieving the global optimal solution. Where the function minimum solution equation of GA is shown in Eq. (10) (Woods et al., 2021).

$$f(x) = -10(\cos 2\pi x_2 + \cos 2\pi x_1) - (-20 - x_1^2 - x_2^2) \quad (10)$$

In Eq. (10), $f(x)$ denotes the minimum value of the function, and x_1 and x_2 denote the values of the horizontal coordinates in the data. When the GA performs the operation, the algorithmic process of the GA is shown in Fig. 2.

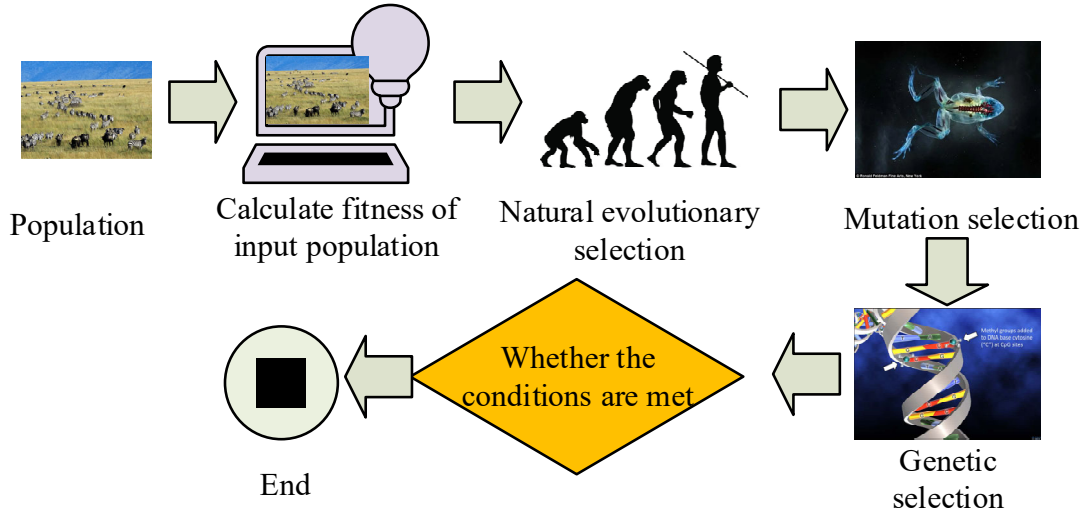


Fig. 2. Basic process of genetic algorithm

As illustrated in Fig. 2, after the initial population is input, the GA assesses whether the operation should be carried out on the data's fitness. If it meets the operation conditions, it proceeds with data selection, cross-mutation, and ultimately concludes with the acquisition of the latest population. Clear and logical steps are taken by the algorithm to ensure optimal results (Woods et al., 2021). The entire algorithmic process revolves around solving the global optimal solution. Although the GA has a good algorithmic advantage in solving the optimal solution, but its algorithm is less efficient, while the calculation will appear premature convergence is not conducive to the detection of concrete damage.

The BPNN model and the GA model are combined in the GA-BP prediction model, a hybrid algorithm model that may use both algorithms to process data for determining the extent of damage and strength of concrete. When generating random BPNN parameter errors, chromosome coding is needed for different populations and different random numbers (Woods et al., 2021). As shown in Eq. (11) (Qin et al., 2021).

$$S = (n + 1) \times l + (l + 1) \times m \quad (11)$$

In Eq. (11), n denotes the number of input nodes, l denotes the number of nodes in the hidden layer. By calculating the fitness of the data can be able to judge the feature extraction and genetic merit of different datasets and individuals. Eq. (12) is the equation for genetic variation and cross replication (Chen, 2022).

$$F = \frac{1}{\sum (\overline{X'_l} - X'_l)^2 + \gamma (\sum_{j=1}^m V_j^2 + \sum_{k=1}^l W_k^2)} \quad (12)$$

In Eq. (12), $\overline{X'_l}$ denotes the average value of the processed data and γ denotes the regularity coefficient. Although the GA-BP algorithm is able to process the data more optimally, but the algorithm still has defects in training and individual optimal solutions. PSO is a search algorithm for the study of bird feeding behavior, which is capable of solving

multi-dimensional problems with multiple stochastic individuals for solving the extremes and calculating the optimal solution. As shown in Eq. (13) (Dou et al., 2022).

$$V_i'' = -c_2 r_2 (g_{best} + X_i)_i + c_1 r_1 (p_i - X_i) + w * V$$

$$X_i'' = V_i'' + X_i$$
(13)

In Eq. (13), V_i'' represents the velocity change of the particle after updating, V_i represents the velocity of the particle before updating, X_i'' represents the position information of the particle updating in the algorithm, X_i represents the position information of the particle before updating, w represents the inertia characteristic coefficient possessed by the particle, c_1 and c_2 represent the parameter values of the learning factor in the algorithm, and r_1 and r_2 represent the random values in the numerical values 0-1. Because the particle swarm algorithm has the capability of global search, it has several advantages when determining the algorithm's best answer (Dhayalan et al., 2020). The creation of the enhanced GA-PSO-BP algorithm model is made possible by including the BPNN encoder on top of the improved GA-PSO algorithm model. The enhanced hybrid algorithm model's flow diagram is depicted in Fig. 3.

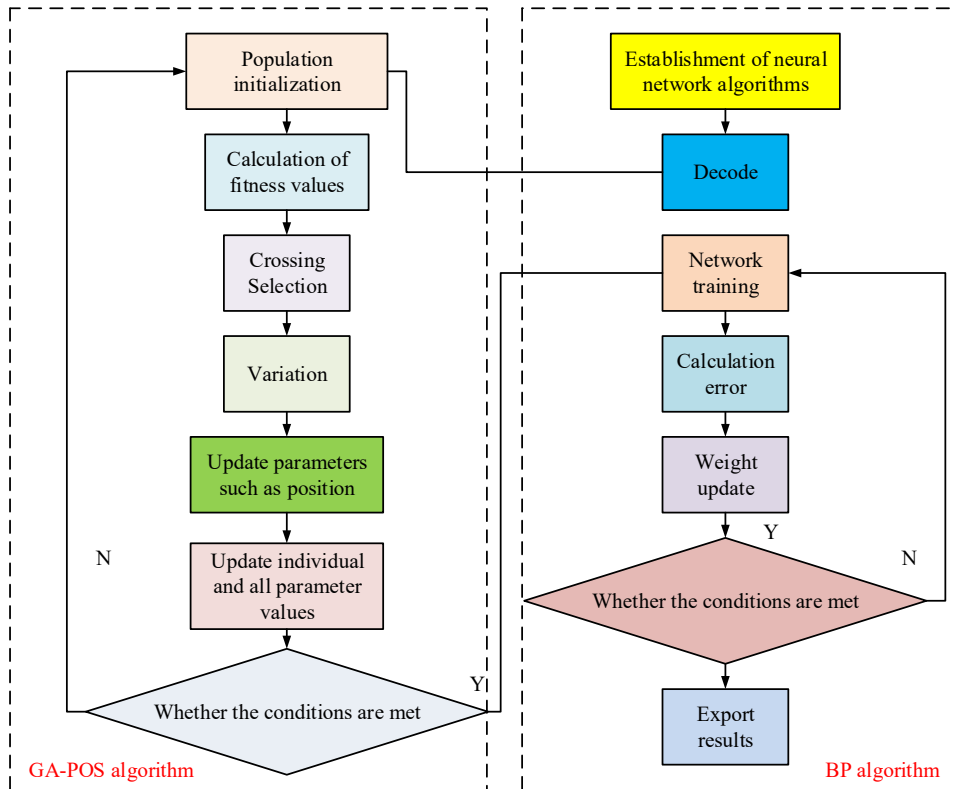


Fig. 3. Improved GA-POS-BP algorithm

In Fig. 3, the hybrid algorithm model combining the three algorithms has more tangible detection advantages than the separate algorithm model. To start, the particle swarm algorithm can be used to select the number of populations, and the optimal solution can be solved for the randomly generated individuals. In the calculation of fitness, the GA can be used to solve the fitness, but the difference with the GA is that the global and individual fitness can be calculated. At the same time, after calculating the influence of individuals and the transmission of genetic material, the calculated information on the number of individuals and the speed of individuals can be updated in different populations of individuals in order to better analyze the location of individuals. The improved GA-PSO-BP algorithm model combines the benefits of the three models, giving it more algorithmic advantages in the detection of concrete loss. By continuously updating weights during training, a more accurate network model can be obtained (Seraj and Evans, 2020). After establishing an improved GA-PSO-BP algorithm model, the current specific data was tested using ultrasonic rebound detection data, and the intensity measurement curve fitted by the model was compared with the ultrasonic rebound comprehensive method. Analyze errors to ascertain accuracy levels and use both fitted and trained data to predict concrete strength and detect any potential damage. The ultrasonic rebound method can be utilized to train the concrete data with algorithmic models. It is important to avoid alternate techniques or scenarios for data training as this can result in unreliable data. Thus, achieving the desired reliability for the ultrasonic rebound method typically requires data training as the only means.

4. Analysis of CDD Experimental Results of Improved GA-PSO-BP Algorithm Model

This study used commonly used materials from cement factories to produce large ready-mixed concrete specimens with different strengths (C20, C25, C30, C40, C50, C60), as well as rebound value detection data of long-term concrete under natural curing at different ages (360d, 730d, 1095d, 2562d, 3400d, 4211d), and established a comprehensive measurement curve for ultrasonic rebound strength of long-term concrete. The strength and compressive values were tested for several different sets of concrete loss levels in the full data, comparing the BPNN model, the GA-BP algorithm model and the improved GA-PSO-BP algorithm model, and were obtained as shown in Table 1.

Table 1. Concrete strength and compressive testing

Serial number	Compressive strength value	Inferred strength value			
		Strength curve	BP model	GA-BP model	GA-PSO-BP model
1	51.2	62.8	63.4	55.62	53.21
2	58.9	58.93	60.3	59.61	59.22
3	42.1	44	44.68	46.46	44.86
4	67.3	65.72	64.98	67.51	66.99
5	71.6	63.01	62.54	66.25	67.98
6	63.2	65.34	66.94	69.57	69.24
7	42.6	48.84	47.99	43.98	41.92
8	58.1	59.34	59.42	62.33	58.61

In Table 1, different compressive strength values produce different wall measurement curves when testing the strength of concrete. Comparing the compressive strength of concrete in the three algorithmic models, it was discovered that the three improved GA-PSO-BP algorithmic models projected strength values closer to the compressive strength values. The fifth specimen tested displayed the highest compressive strength value among the samples. This result can be attributed to the varying age of the concrete samples. However, among the three algorithmic models, the enhanced GA-PSO-BP algorithm is better equipped to measure the extent of concrete loss and exhibits a relatively higher level of accuracy. Fig. 4 compares the root mean square error curves for all three algorithms.

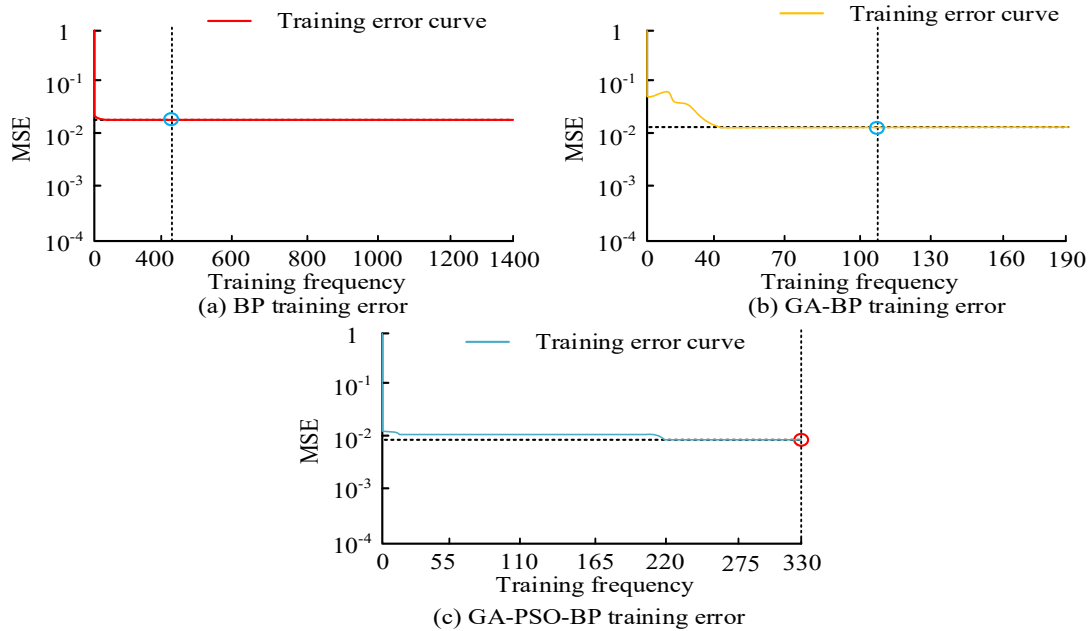


Fig. 4. Comparison of Root-mean-square deviation curves of three algorithms

The BPNN model in Fig. 4 modifies the number of training times to reach 410 when the training error approaches the convergence state, with an overall algorithm test error value of about 0.017. The GA-BP algorithm reaches the optimal error at the number of training times of 190 at this time the error value of 0.010, and at the number of training times of 105 when the error reaches the convergence state. When the algorithm has been trained 330 times, the ideal error for the enhanced GA-PSO-BP algorithm is reached. At this point, the error value is 0.009, and the error has converged. It is clear that the enhanced GA-PSO-BP algorithm outperforms the other two algorithms in terms of root mean square error, which is lower than both the BPNN's 0.008 and the GA-BP method's 0.001. The actual and predicted values of the three algorithms for testing the degree of damage to the concrete are compared to obtain the curves shown in Fig. 5.

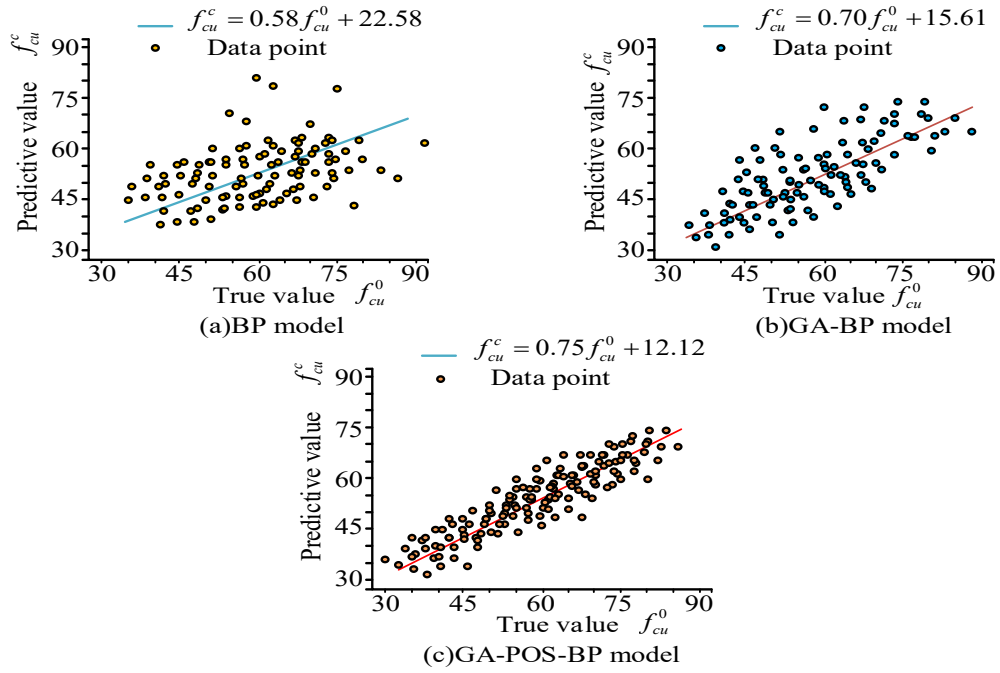


Fig. 5. Real and predicted values of three algorithms

The enhanced GA-PSO-BP method in Fig. 5 has the highest slope of the curve; the points of various training test degrees are located nearer to the curve; at this point, the curve parameter's value is 0.75. The slope of the curve for the GA-BP algorithm model is exceedingly low at just 0.70, which is lower than even the IA model at 0.05. Further, the BPNN algorithm model has an even lower slope at 0.58, again lower than the IA model at 0.17. Overall, the curve strength of the IA model is higher than that of the other two models. This indicates that the IA's model is significantly more thoroughly tested, as the other two algorithms exhibit more discrete test values relative to the curve. The stability and accuracy of the algorithms will be assessed after the performance of the algorithms for concrete detection to confirm how well the algorithms perform in various scenarios. A comparison chart of the three algorithms' accuracy may be shown in Fig. 6.

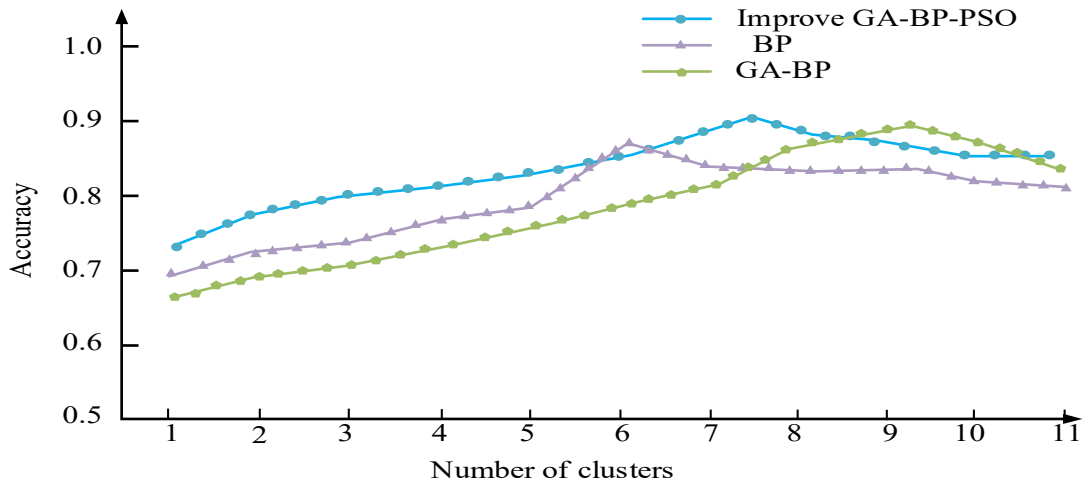


Fig. 6. Comparison of algorithm accuracy

In Fig. 6, the accuracy of the three algorithms increases with the number of training samples. However, the accuracy of the algorithms shows a decreasing trend once it reaches the maximum value, as the number of samples increases. When there are seven samples, the accuracy of IA is at its highest, 0.91. When there are 6 samples, the accuracy of BPNN is 0.84, and when there are 9 samples, the accuracy of the GA-BP method is 0.89. The accuracy of the IA algorithm is the highest of the three, surpassing the BP algorithm model's accuracy by 0.07 and the GA-BP algorithm model's accuracy by 0.02. It is clear that IA outperforms the conventional algorithm model in terms of algorithmic model correctness. In Fig. 7, the three algorithms' test set and training set accuracy are contrasted.

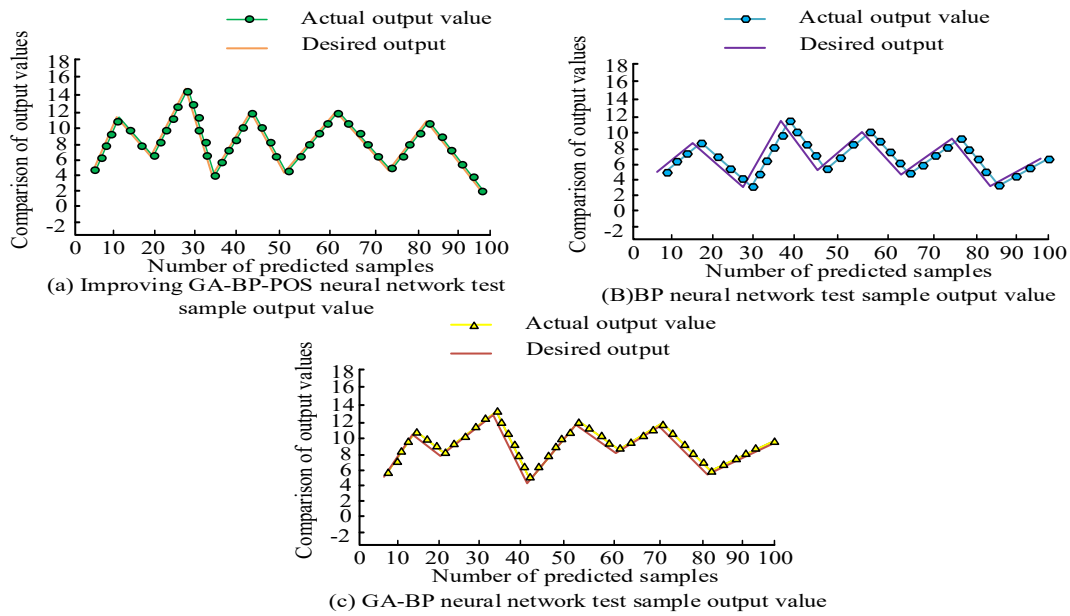


Fig. 7. Comparison of the accuracy of three algorithms

The anticipated and true values for the three algorithms in Fig. 10 exhibit an upward and downward trend as the number of training sessions rises. The accuracy of IA is currently 95.61%. However, the accuracy of the other two algorithms, BPNN and GA-BP, has a relatively large deviation of the curve of the predicted and true value, with an accuracy of 89.52% and 92.68%, respectively. This indicates that the algorithm of this algorithm has a high accuracy of algorithmic testing. The accuracy of the two algorithms is worse than IA by 6.09% and 2.93%, respectively, making them even less accurate than IA. This demonstrates that IA has higher algorithmic accuracy than the conventional algorithm model.

5. Discussion

With the rapid development of the construction industry in the national economy, the production of concrete has also grown rapidly, and the aging problem of concrete in some elderly buildings has gradually become prominent. The traditional inspection and maintenance of long-term concrete can cause varying degrees of damage to the concrete, so it is necessary to put forward stricter requirements for the current inspection technology. This study established a new improved GA-PSO-BP algorithm and ultrasonic rebound detection of concrete damage. When testing the strength and other properties of concrete, the improved GA-PSO-BP algorithm had a small deviation between the compressive strength curve and the real curve, and the numerical values were basically close to the real curve. The better data processing and optimization of the improved GA-PSO-BP algorithm may account for its superior performance compared to the other two algorithm models. Upon comparison of the root mean square error between the three algorithms, the error value of the improved GA-PSO-BP algorithm was found to be smaller. However, the GA-PSO-BP algorithm required higher training frequency in comparison to the GA-BP algorithm. However, the training error value of the GA-BP algorithm was larger, indicating that the GA-BP algorithm reached the local limit during training, resulting in shorter training data time and early termination of training. At the same time, the training value and error effect of the BP algorithm were the worst. Comparing the differences between the true and predicted values of the three models, it was observed that the improved GA-PSO-BP algorithm had a closer curve change trend to the true value. This indicated that the improved GA-PSO-BP algorithm had a better prediction performance than the other two algorithms, and could better help the current model data to achieve convergence.

When comparing the accuracy change curves of the three algorithms, the change curves of the three algorithms increased with the increase of the number of samples trained, but all showed a decreasing trend in accuracy when reaching a certain number. The sample training accuracy curve value of the improved GA-PSO-BP algorithm was the highest, and the number of samples was the largest when the accuracy decreases. This may be because the improved GA-PSO-BP algorithm model was more stable when training samples, and its training curve was more in line with the real curve. When testing the accuracy of the three algorithms, the expected values and actual output curves of the three algorithms fluctuated up and down with the increase of sample size. However, the trend of the improved GA-PSO-BP algorithm was close to the actual output curve, indicating that the algorithm was closer to the actual output curve when training sample data. It was possible to improve the GA-PSO-BP algorithm by integrating the advantages of the other two algorithms during training, resulting in better training of the algorithm.

In summary, the improved GA-PSO-BP algorithm outperforms the other two algorithms in terms of algorithm performance and processing of current concrete data. This indicates that the IA model can improve the accuracy and accuracy of current data prediction, indicating that the algorithm performs better in processing concrete damage data.

6. Conclusion

The research first establishes the concrete data using the UR technique, compares multiple algorithms to produce a hybrid algorithm model based on DL, and then analyses the concrete loss data using the IA model. The experimental findings showed that the hybrid IA was more precise and accurate than the conventional algorithm model. The root mean square error of IA was lower compared to the two algorithms, being less than the BPNN 0.008 and less than the GA-BP algorithm 0.001. IA was also superior to the traditional algorithm in detecting the degree of concrete loss, with tighter detection curve points. The accuracy of IA was lower compared to the two traditional algorithms, where it was lower than IA by 6.09% and 2.93%. It performed better than the BP algorithm model and the GA-BP algorithm model by 0.07 and 0.02, respectively, making it the highest of the three algorithms. IA had a more stable algorithm than the traditional method, and both methods had a reduced loss function. A new algorithm for detecting the degree of concrete loss had been developed as a result of this research, which addressed the CDD algorithm's lack of precision and accuracy. However, the research still has many issues, and additional concrete data will be evaluated in the future. The complexity of predicting the long-term strength of concrete has prompted research to conduct experiments only by considering some long-term concrete influencing factors, despite considering incomplete factors. Future research directions will also involve in-depth examination of the correlation analysis between age and grey correlation, determination of the equation for the long-term concrete strength curve with age as the independent variable, and adjustment of parameters for the strength measurement curve. Through trial and error in adjusting the spatial structure of the neural network model, further optimization can be achieved. In addition to utilizing the enhanced GA-PSO optimization algorithm to fine-tune the BP network, other algorithms can also be experimented with for training optimization of the BP network, without being restricted solely to adjusting the connection strength.

Funding

The research is supported by 2022 Nantong Basic Science Research and Social Livelihood Science and Technology Plan Project, Durability Research of Steel Slag Recycled concrete prefabricated revetment structure (MSZ2022197); 2022 Nantong Basic Science Research and Social Livelihood Science and Technology Plan Project, Research on Corrosion Performance of Precast and Fabricated Bank Protection Concrete Structure in chlorine Environment (JCZ2022111).

Institutional Review Board Statement

Not applicable.

References

- Bhowmick, S. and Nagarajaiah, S. (2020). Automatic detection and damage quantification of multiple cracks on concrete surface from video. *International Journal of Sustainable Materials and Structural Systems*, 4(2/3/4), 292. doi:10.1504/IJSMSS.2020.109097.
- Chen, Z. (2022). Research on internet security situation awareness prediction technology based on improved RBF neural network algorithm. *Journal of Computational and Cognitive Engineering*, 1(3), 103-108. doi:10.1016/j.jcce.2021.11.005.
- Dhyalalan, R., Saravanan, S., Manivannan, S., and Rao, B. Purna Chandra. (2020). Development of ultrasonic waveguide sensor for liquid level measurement in loop system. *Electronics Letters*, 56(21), 1120-1122. doi:10.1049/el12072.
- Dou, P., Jia, Y., Zheng, P., and Wu, T. (2022). Review of ultrasonic-based technology for oil film thickness measurement in lubrication. *Tribology International*, 165 (1), 107-122. doi:10.1016/j.triboint.2021.107122.
- Fang, L., Zhou, Y., Jiang, Y., Pei, Y., and Yi, W. (2020). Vibration-based damage detection of a steel-concrete composite slab using non-model-based and model-based methods. *Advances in Civil Engineering*, 2020 (2), 1-20. doi:10.1155/2020/8884823.
- Gao, W., Kong, Q., Lu, W., and Lu, X. (2022). High spatial resolution imaging for damage detection in concrete based on multiple wavelet decomposition. *Construction and Building Materials*, 319(8), 10-18. doi:10.1016/j.conbuildmat.2021.126057.
- Jesús, N. E., Cédric, P., Rakotonarivo, S., and Garnier, V. (2021). Damage detection and localization from linear and nonlinear global vibration features in concrete slabs subjected to localized thermal damage. *Structural Health Monitoring*, 20(2), 567-579. doi:10.1177/1475921720941792.
- Karve, P., Miele, S., Neal, K., Mahadevan, S., Agarwal, V., Giannini, E. R., and Kyslinger, P. (2020). Vibro-acoustic modulation and data fusion for localizing alkali-silica reaction-induced damage in concrete. *Structural Health Monitoring*, 19(6), 1905-1923. doi:10.1177/1475921720905509.
- Lin, F. and Scherer, R. J. (2020). Concrete bridge damage detection using parallel simulation. *Automation in Construction*, 119(10), 1-14. doi:10.1016/j.autcon.2020.103283.
- Lin, S. T. K., Lu, Y., Alamdari, M. M., and Khoa, N. L. D. (2020). Field test investigations for condition monitoring of a concrete culvert bridge using vibration responses. *Structural Control and Health Monitoring*, 27(3), 2-18. doi:10.1002/stc.2274.
- Nasery, M. M., Husem, M., Okur, F. Y., Altunisik, A. C., and Nasery, M. E. (2020). Model updating - based automated damage detection of concrete cased composite column - beam connections. *Structural Control and Health Monitoring*, 27(10), e2600. doi:10.1002/stc.2600.
- Pan, X. and Yang, T. Y. (2020). Postdisaster image - based damage detection and repair cost estimation of reinforced concrete buildings using dual convolutional neural networks. *Computer - Aided Civil and Infrastructure Engineering*, 35(5), 495-510. doi:10.1111/mice.12549.

- Peng, X., Qin, F. J., Yang, Q. W., and Chen, H. (2021). A Robust Estimate Method for Damage Detection of Concrete Structures Using Contaminated Data. *Advances in Civil Engineering*, 2021(5), 1-13. doi:10.1155/2021/6669958.
- Qi, A. and Chen, P. (2022). Damage and crack detection of self-compacting concrete based on fuzzy analytic hierarchy process. *International Journal of Materials and Product Technology*, 64(4), 292-306. doi:10.1016/S0923-4748(22)00006-1.
- Qin, Y., Duan, M., Ma, W., Li, Y., Zhou, H., Lv, Y., and Li, M. (2021). Experimental study on the damage permeability of polypropylene fiber-reinforced concrete. *Construction and Building Materials*, 286(4), 20-29. doi:10.1016/j.conbuildmat.2021.121747.
- Scherr, J. F. and Grosse, C. U. (2020). Delamination detection on a concrete bridge deck using impact echo scanning. *Structural Concrete*, 22(2), 806-812. doi:10.1002/suco.201900159.
- Van Steen, C., Nasser, H., Verstryngge, E., and Wevers, M. (2021). Acoustic emission source characterization of chloride-induced corrosion damage in reinforced concrete. *Structural Health Monitoring*, 34(3), 1266-1286. doi:10.1177/1475921720978886.
- Woods, J. E., Yang, Y. S., Chen, P. C., Lau, D. T., and Erochko, J. (2021). Automated crack detection and damage index calculation for RC structures using image analysis and fractal dimension. *Journal of Structural Engineering*, 147(4), 5-19. doi:10.1061/(ASCE)ST.1943-541X.0002995.
- Yin, T., Ng, C. T., and Kotousov, A. (2021). Damage detection of ultra-high-performance fibre-reinforced concrete using a harmonic wave modulation technique. *Construction and Building Materials*, 313(11), 3-16. doi:10.1016/j.conbuildmat.2020.121382.
- Zhang, C., Chang, C., and Jamshidi, M. (2020). Concrete bridge surface damage detection using a single-stage detector. *Computer-Aided Civil and Infrastructure Engineering*, 35(4), 389-409. doi:10.1111/mice.12500.
- Zima, B. and Krajewski, M. (2022). The vibration-based assessment of the influence of elevated temperature on the condition of concrete beams with pultruded GFRP reinforcement. *Composite Structures*, 282(Feb.), 11-23. doi:10.1016/j.compstruct.2021.117898.
- Znidaric, A., Kreslin, M., and Anzlin, A. (2020). Detection of delaminated and cracked concrete with unmanned aerial vehicles. *Routes Roads*, 36(3), 29-32. doi:10.1080/14622010.2019.1655556.



Suzheng Zhao obtained his master's degree in civil engineering (2008) from Nanjing Forestry University. Presently, he is working as a Senior Technician and First level construction engineer Lecturer, and the Dean of the Department of Civil Engineering Teaching and Research Office at the School of Shipbuilding and Ocean Engineering at Jiangsu Shipping Vocational and Technical College. He has been invited as a resource person to give various technical talks on concrete material performance research, construction safety management, and image processing in civil engineering. He has published articles in 18 well-known journals, and his areas of interest include image processing, concrete durability experiments, and experimental research on concrete mechanical properties.